October 1, 2008

Multiplexed Screening of Cellular Uptake of Gold Nanoparticles Using Laser Desorption/Ionization Mass Spectrometry

ZJ Zhu
PS Ghosh
OR Miranda
RW Vachet
VM Rotello

J|A|C|S
ARTICLES

Published on Web 10/01/2008

Multiplexed Screening of Cellular Uptake of Gold Nanoparticles Using Laser Desorption/Ionization Mass Spectrometry

Zheng-Jiang Zhu, Partha S. Ghosh, Oscar R. Miranda, Richard W. Vachet,* and Vincent M. Rotello*

Department of Chemistry, University of Massachusetts, Amherst, Massachusetts 01003

Received February 7, 2008; E-mail: rotello@chem.umass.edu (V.M.R.); rwvachet@chem.umass.edu (R.W.V.)

Abstract: Gold nanoparticles (AuNPs) are highly promising candidates as drug delivery agents into cells of interest. We describe for the first time the multiplexed analysis of nanoparticle uptake by cells using mass spectrometry. We demonstrate that the cellular uptake of functionalized gold nanoparticles with cationic or neutral surface ligands can be readily determined using laser desorption/ionization mass spectrometry of cell lysates. The surface ligands have "mass barcodes" that allow different nanoparticles to be simultaneously identified and quantified at levels as low as 30 pmol. Using this method, we find that subtle changes to AuNP surface functionalities can lead to measurable changes in cellular uptake propensities.

Introduction

Therapeutic nanocarriers carry drugs, genes, and/or imaging agents into cells and tissues of interest.[1−4] Various materials, such as polymeric micelles,[5] mesoporous silica nanorods,[6] carbon nanotubes,[7] and nanoparticles,[8−10] have been used as therapeutic nanocarriers, as well as probes for following intracellular processes. Effective use of nanoparticles as carriers and intracellular probes requires the ability to monitor these particles in cells, and several techniques are available for this purpose. These techniques can be classified into two groups: (1) label-free imaging techniques such as luminescent quantum dots imaging,[10,11] atomic force microscopy (AFM),[12] and transmission electron microscopy (TEM)[13] and (2) barcoding techniques such as those that encode nanoparticles with fluorescence dyes that can be "read out" by a fluorescence spectrometer.[2] Simultaneous screening of the cellular uptake of multiple particles with different surface functional groups, however, is a challenge for existing approaches. Here, we describe a new "mass barcoding" technique for monitoring the cellular uptake of multiple functionalized gold nanoparticles (AuNPs) by using laser desorption/ionization mass spectrometry (LDI-MS).

Nanoparticles have been used in mass spectrometric analyses primarily to facilitate the laser desorption/ionization of compounds of interest. Tanaka et al.[14] showed that cobalt particles (∼30 nm) suspended in glycerol facilitated the ionization of proteins. Subsequently, Ag,[15] Au,[16−22] C,[23] and Si[24,25] nanomaterials have been demonstrated as LDI-MS matrixes with different degrees of success. Meanwhile, some mass spectrometric work has also been devoted to the analysis of nanoparticles themselves. For pure samples of gold nanoparticles, electrospray ionization mass spectrometry (ESI-MS)[26,27] and

(1) Peer, D.; Karp, J. M.; Hong, S.; Farokhzad, O. C.; Margalit, R.; Langer, R. *Nat. Nanotechnol.* **2007**, *2*, 751–760.
(2) Rosi, N. L.; Giljohann, D. A.; Thaxton, C. S.; Lytton-Jean, A. K. R.; Han, M. S.; Mirkin, C. A. *Science* **2006**, *312*, 1027–1030.
(3) Michalet, X.; Pinaud, F. F.; Bentolila, L. A.; Tsay, J. M.; Doose, S.; Li, J. J.; Sundaresan, G.; Wu, A. M.; Gambhir, S. S.; Weiss, S. *Science* **2005**, *307*, 538–544.
(4) Han, G.; You, C.-C.; Kim, B.-J.; Turingan, R. S.; Forbes, N. S.; Martin, C. T.; Rotello, V. M. *Angew. Chem., Int. Ed.* **2006**, *45*, 3165–3169.
(5) Savic, R.; Luo, L.; Eisenberg, A.; Maysinger, D. *Science* **2003**, *300*, 615–618.
(6) Giri, S.; Trewyn, B. G.; Stellmaker, M. P.; Lin, V. S. Y. *Angew. Chem., Int. Ed.* **2005**, *44*, 5038–5044.
(7) Kam, N. W. S.; O'Connell, M.; Wisdom, J. A.; Dai, H. *Proc. Natl. Acad. Sci. U.S.A.* **2005**, *102*, 11600–11605.
(8) Hong, R.; Han, G.; Fernandez, J. M.; Kim, B.-J.; Forbes, N. S.; Rotello, V. M. *J. Am. Chem. Soc.* **2006**, *128*, 1078–1079.
(9) Lewin, M.; Carlesso, N.; Tung, C.-H.; Tang, X.-W.; Cory, D.; Scadden, D. T.; Weissleder, R. *Nat. Biotechnol.* **2000**, *18*, 410–414.
(10) Gao, X.; Cui, Y.; Levenson, R. M.; Chung, L. W. K.; Nie, S. *Nat. Biotechnol.* **2004**, *22*, 969–976.
(11) Jaiswal, J. K.; Mattoussi, H.; Mauro, J. M.; Simon, S. M. *Nat. Biotechnol.* **2003**, *21*, 47–51.
(12) Yang, P. H.; Sun, X.; Chiu, J. F.; Sun, H.; He, Q. Y. *Bioconjugate Chem.* **2005**, *16*, 494–496.
(13) Chithrani, B. D.; Ghazani, A. A.; Chan, W. C. W. *Nano Lett.* **2006**, *6*, 662–668.
(14) Tanaka, K.; Waki, H.; Ido, Y.; Akita, S.; Yoshida, Y.; Yoshida, T.; Matsuo, T. *Rapid Commun. Mass Spectrom.* **1988**, *2*, 151–153.
(15) Owega, S.; Lai, E. P. C.; Bawagan, A. D. O. *Anal. Chem.* **1998**, *70*, 2360–2365.
(16) Novikov, A.; Caroff, M.; Della-Negra, S.; Lebeyec, Y.; Pautrat, M.; Schultz, J. A.; Tempez, A.; Wang, H. Y. J.; Jackson, S. N.; Woods, A. S. *Anal. Chem.* **2004**, *76*, 7288–7293.
(17) McLean, J. A.; Stumpo, K. A.; Russell, D. H. *J. Am. Chem. Soc.* **2005**, *127*, 5304–5305.
(18) Castellana, E. T.; Russell, D. H. *Nano Lett.* **2007**, *7*, 3023–3025.
(19) Huang, Y. F.; Chang, H. T. *Anal. Chem.* **2006**, *78*, 1485–1493.
(20) Su, C. L.; Tseng, W. L. *Anal. Chem.* **2007**, *79*, 1626–1633.
(21) Nagahori, N.; Nishimura, S.-I. *Chem.—Eur. J.* **2006**, *12*, 6478–6485.
(22) Spencer, M. T.; Furutani, H.; Oldenburg, S. J.; Darlington, T. K.; Prather, K. A. *J. Phys. Chem. C* **2008**, *112*, 4083–4090.
(23) Sunner, J.; Dratz, E.; Chen, Y.-C. *Anal. Chem.* **1995**, *67*, 4335–4342.
(24) Wei, J.; Buriak, J. M.; Siuzdak, G. *Nature* **1999**, *399*, 243–246.
(25) Northen, T. R.; Yanes, O.; Northen, M. T.; Marrinucci, D.; Uritboonthai, W.; Apon, J.; Golledge, S. L.; Nordstrom, A.; Siuzdak, G. *Nature* **2007**, *449*, 1033–1036.
(26) Tracy, J. B.; Kalyuzhny, G.; Crowe, M. C.; Balasubramanian, R.; Choi, J. P.; Murray, R. W. *J. Am. Chem. Soc.* **2007**, *129*, 6706–6707.

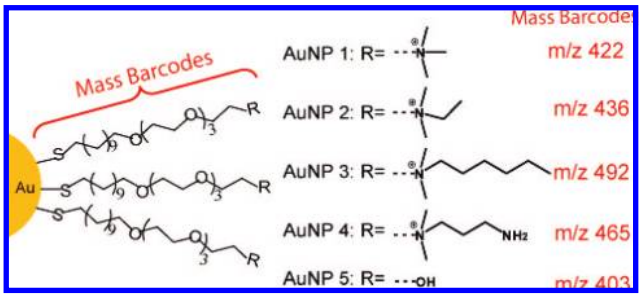

Figure 1. Structural representation of the AuNPs. The mass/charge ratios (*m*/*z*) attached to each AuNP act as mass barcodes used for identification of the AuNPs.

LDI-MS[28,29] have been used to measure the compositions of surface functionalities and atom numbers in the NP core.

In this study, we have tagged AuNPs with readily ionizable surface functionalities, i.e., "mass barcodes" (shown in Figure 1). These alkanethiolate cationic or neutral monolayers are barriers between the nanoparticle core and the environment, effectively protecting and stabilizing the gold cluster core in biological environments.[30−32] Moreover, the chemical nature of these monolayers dictates interfacial interactions between cells and AuNPs, thus governing cellular uptake of AuNPs.[33−35] Upon laser irradiation of these AuNPs, mass barcodes of alkanethiolate monolayers rather than the AuNPs themselves can be simply read out by LDI-MS, thus providing characteristic peaks for identifying AuNPs (e.g., Figure S1 in the Supporting Information, LDI-MS spectrum of AuNP **1**). Ionization of alkanethiolate monolayers on flat gold surfaces has also been observed using LDI[36,37] and matrix-assisted LDI (MALDI).[38,39] The surface ligands on the AuNPs are primarily detected because the NP core efficiently absorbs the laser light (337 nm), and this energy is readily transferred to desorb and ionize the surface ligands, probably via a mechanism similar to that proposed by Tanaka.[14] In this work, we investigate a potential advantage of such a mass barcoding approach—the ability to simultaneously analyze many different functionalized AuNPs. We predicted that each functionalized AuNP could be identified by its unique mass barcode. Furthermore, we explore this LDI strategy for direct analyses of AuNPs taken up by cells. Such a multiplexed screening of AuNPs could be very valuable for rapidly assessing the chemical and physical parameters that influence AuNP uptake by cells. To the best of our knowledge, this is the first report of multiplexed analysis of cellular uptake of functionalized AuNPs with LDI-MS.

Results and Discussion

To explore the viability of mass barcodes for determining the uptake efficiency of AuNPs, we cultured monkey kidney cells (COS-1) with AuNPs (500 nM) for 6 h (Figure 2a). This concentration of AuNPs is nontoxic to the cells,[40] and after 6 h of incubation, no cell morphology changes are observed. The cells were washed three times with cold phosphate-buffered saline (PBS) to remove extra AuNPs that were not taken up by the cells. Before the cells were lysed, TEM was used to verify the cellular uptake of AuNPs. As shown for a single cell (Figure 2b), multiple gold nanoparticles are trapped in vesicles (most likely via endosomal entrapment) in the cytoplasm, which is in agreement with results by other groups.[13,41,42] It is possible that some AuNPs have escaped from the vesicles, as NP escape depends on the NP surface functionalities,[42,43] but direct evidence for this was not found in the TEM images. After the cells were lysed, the AuNPs taken up by the cells were then collected as part of the precipitate after centrifugation of the lysate. The precipitate was subjected to LDI-MS, and spectra similar to that shown in Figure 3a were obtained. Figure 3a illustrates the characteristic peaks that are observed for AuNP **1**. The spectrum of AuNP **1** includes an ion at *m*/*z* 422, which corresponds to the molecular ion (M^+) of the ligand attached to AuNP **1**. The spectrum also includes ions at *m*/*z* 388, which corresponds to $[M - H_2S]^+$, *m*/*z* 197 and 394, which correspond to Au^+ and Au_2^+, respectively, and *m*/*z* 184, which corresponds to the headgroup fragment of one of the most abundant lipids in animal cell membranes—phosphatidylcholine (PC). Moreover, a series of peaks spaced by 14 Da from *m*/*z* 262 to *m*/*z* 360 indicate successive losses of CH_2 units from the alkyl chains of the surface ligands. Each of the other AuNPs in this study had similar mass spectral patterns, with each AuNP featuring different *m*/*z* ratios allowing identification (Figure S2 in the Supporting Information).

The different mass barcodes of each AuNP facilitate multiplexed screening by LDI-MS. After cells are simultaneously exposed to two different types of AuNPs, LDI-MS analysis of the resulting cell lysate indicates that both AuNPs can be readily identified. For example, in Figure 3b, diagnostic molecular ions at *m*/*z* 422 and *m*/*z* 436 indicate the cellular uptake of AuNP **1** and AuNP **2**, respectively. Other characteristic peaks, such as $[M - H_2S]^+$ (*m*/*z* 388 for AuNP **1** and *m*/*z* 402 for AuNP **2**), also assist the identification of two AuNPs.

Quantifying the relative cellular uptake of these two different AuNPs should be possible by comparing the ion abundances of their respective molecular ion peaks. To do so, however, the relative ionization efficiencies of the ligands in cell lysates must be considered. The ionization efficiencies of the surface ligands were investigated under two sets of control conditions. First, equal molar amounts of AuNP **1** and AuNP **2** (300 pmol each) were directly analyzed by LDI-MS, indicating that the ligands

(27) Tracy, J. B.; Crowe, M. C.; Parker, J. F.; Hampe, O.; Fields-Zinna, C. A.; Dass, A.; Murray, R. W. *J. Am. Chem. Soc.* **2007**, *129*, 16209–16215.
(28) Schaaff, T. G. *Anal. Chem.* **2004**, *76*, 6187–6196.
(29) Tsunoyama, H.; Negishi, Y.; Tsukuda, T. *J. Am. Chem. Soc.* **2006**, *128*, 6036–6037.
(30) Templeton, A. C.; Wuelfing, W. P.; Murray, R. W. *Acc. Chem. Res.* **2000**, *33*, 27–36.
(31) Kanaras, A. G.; Kamounah, F. S.; Schaumburg, K.; Kiely, C. J.; Brust, M. *Chem. Commun.* **2002**, 2294–2295.
(32) You, C.-C.; Miranda, O. R.; Gider, B.; Ghosh, P. S.; Kim, I.-B.; Erdogan, B.; Krovi, S. A.; Bunz, U. H. F.; Rotello, V. M. *Nat. Nanotechnol.* **2007**, *2*, 318–323.
(33) Leroueil, P.; Hong, S.; Mecke, A.; Baker, J.; Orr, B.; Banaszak Holl, M. *Acc. Chem. Res.* **2007**, *40*, 335–342.
(34) Sandhu, K. K.; McIntosh, C. M.; Simard, J. M.; Smith, S. W.; Rotello, V. M. *Bioconjugate Chem.* **2002**, *13*, 3–6.
(35) Xu, Z. P.; Zeng, Q. H.; Lu, G. Q.; Yu, A. B. *Chem. Eng. Sci.* **2006**, *61*, 1027–1040.
(36) Trevor, J. L.; Lykke, K. R.; Pellin, M. J.; Hanley, L. *Langmuir* **1998**, *14*, 1664–1673.
(37) Gong, W.; Elitzin, V. I.; Janardhanam, S.; Wilkins, C. L.; Fritsch, I. *J. Am. Chem. Soc.* **2001**, *123*, 769–770.
(38) Su, J.; Mrksich, M. *Langmuir* **2003**, *19*, 4867–4870.
(39) Mrksich, M. *ACS Nano* **2008**, *2*, 7–18.
(40) Goodman, C. M.; McCusker, C. D.; Yilmaz, T.; Rotello, V. M. *Bioconjugate Chem.* **2004**, *15*, 897–900.
(41) Jiang, W.; Kim, B. Y. S.; Rutka, J. T.; Chan, W. C. W. *Nat. Nanotechnol.* **2008**, *3*, 145–150.
(42) Nativo, P.; Prior, I. A.; Brust, M. *ACS Nano* **2008**, *2*, 1639–1644.
(43) Yezhelyev, M. V.; Qi, L.; O'Regan, R. M.; Nie, S.; Gao, X. *J. Am. Chem. Soc.* **2008**, *130*, 9006–9012.

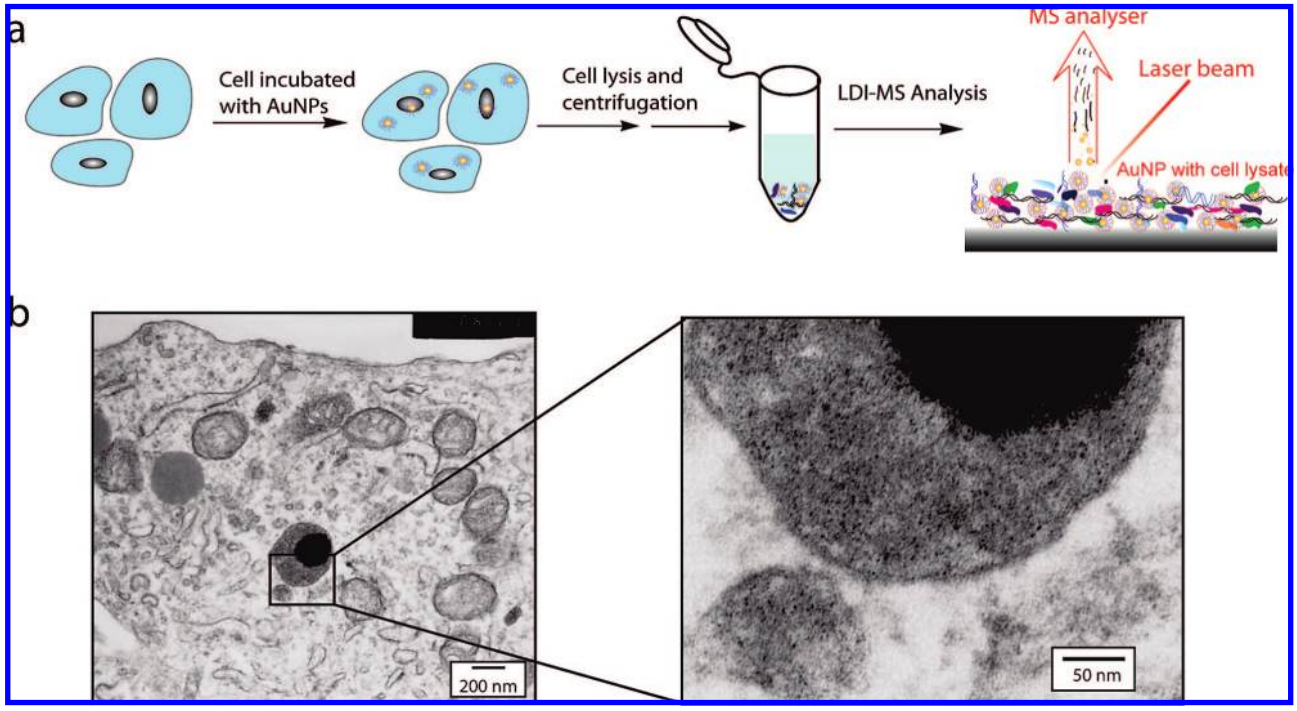

Figure 2. (a) Schematic illustration of the analysis of the AuNPs in cell lysates by LDI-MS. (b) TEM images of cellular uptake of AuNP **1**.

Table 1. LDI-MS Relative Quantification of Cellular Uptake of AuNPs **1**−**5**

	mass barcodes (*m*/*z*)	control ratio[a]	experimental ratio[b]	relative ratio[c]
AuNP **2**/AuNP **1**	436/422	1.41 ± 0.09	1.70 ± 0.14	1.21 ± 0.13
AuNP **3**/AuNP **1**	492/422	0.72 ± 0.08	0.40 ± 0.10	0.50 ± 0.20
AuNP **4**/AuNP **1**	465/422	0.19 ± 0.05	0.21 ± 0.03	1.10 ± 0.30
AuNP **5**/AuNP **1**	369/388	0.26 ± 0.05	0.09 ± 0.02	0.34 ± 0.09

[a] A 300 pmol sample of each AuNP was mixed with 300 pmol of AuNP **1** in lysed COS-1 cells and subjected to LDI-MS analysis. [b] A 300 pmol sample of each AuNP was mixed with 300 pmol of AuNP **1** and then cultured with living COS-1 cells. These cells were then washed, lysed, and analyzed by LDI-MS. [c] Relative ratios are generated by comparing experimental ratios with control ratios.

on AuNP **2** are ionized more readily as indicated by a molecular ion abundance ratio (AuNP **2**/AuNP **1**) of 1.79 ± 0.04. Second, equal molar amounts of AuNP **1** and AuNP **2** (300 pmol each) were mixed with cell lysates and analyzed by LDI-MS, and again, the surface ligands on AuNP **2** are more readily ionized, giving rise to a molecular ion abundance ratio (AuNP **2**/AuNP **1**) of 1.41 ± 0.09 (Table 1 and Figure S3a in the Supporting Information). Because the data from the second set of experiments are more comparable to the cell uptake experiments, the ion abundance ratio of 1.41 can be used to determine the relative quantity of the AuNPs taken up by the cells. After correction of the experimentally observed ratio of 1.70 ± 0.14 (Figure 3b and Table 1) by the ratio observed from the analysis of the cell lysates, the cellular uptake of AuNP **2** was determined to be 1.21 (±0.13) times greater than that of AuNP **1**. A similar analysis can be done for each of the other AuNPs in comparison to AuNP **1** (Figure 4 and Table 1).

The relative uptake amounts of each AuNP provided by the LDI-MS data was validated using inductively coupled plasma mass spectrometry (ICP-MS). ICP-MS provides high sensitivity and robustness for elemental analysis,[13] but it lacks the capacity to identify AuNPs with different surface functionalities. Therefore, the cellular uptake amounts of each AuNP had to be determined separately (see the Experimental Section for details). The relative uptake amounts for each AuNP (compared to AuNP **1**) as determined by ICP-MS (Figure 4 and Table S1 in the Supporting Information) are very similar to the LDI-MS data, indicating that LDI-MS can reliably provide the relative quantities of each AuNP taken up by COS-1 cells. Interestingly, the similarity of the ICP-MS data, which were acquired after uptake of individual AuNPs, and the LDI-MS data, which were acquired after uptake of two different AuNPs, indicates that interactions between the AuNPs in the cell uptake experiments are minimal.

Taken as a whole, the quantitative data in Figure 4 indicate that AuNP **2** and AuNP **4** are more readily taken up by COS-1 cells than AuNP **3** and AuNP **5**. The exact mechanism by which the AuNPs are taken up by the cells is probably complex and is still an active area of investigation. Nonetheless, several factors have been recognized to govern the cellular uptake efficiency of nanoparticles, such as size,[13,41] shape,[13] and surface properties.[12,33−35] Because the cell membrane is negatively charged, positively charged nanoparticles are generally found to have higher uptake efficiencies.[33,35] Therefore, it is perhaps not surprising that AuNP **5** with its neutral surface is less readily taken up by the cells than the cationic AuNPs **1**−**4**.[33,35] While taken up more efficiently than AuNP **5**, the four cationic NPs (AuNP **1** through AuNP **4**) all exhibit slightly different uptake efficiencies. From this limited set of AuNPs, it is difficult to conclude what other factors control uptake, but surface ligand hydrophobicity might be important. AuNP **3** is the most hydrophobic of the cationic AuNPs, and it is least efficiently taken up by the COS-1 cells. Obviously, more work is needed to better understand the effect of hydrophobicity on AuNP cell uptake, and this mass barcode approach along with LDI-MS detection will be helpful in this regard.

To ensure that the results in Table 1 and Figure 4 do not simply reflect different AuNP stabilities in a cellular environment, the AuNPs were kept in cell lysate for different periods

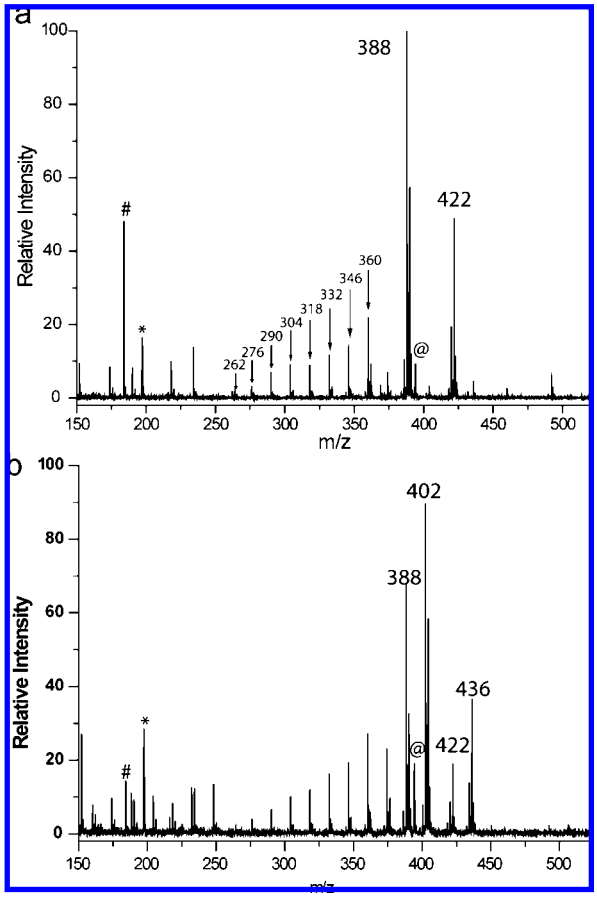

Figure 3. LDI mass spectrum of COS-1 cell lysate after uptake of (a) AuNP **1** and (b) AuNP **1** and AuNP **2**. *m/z* 422 and *m/z* 436 correspond to the molecular ion (M^+) of the ligands attached to AuNP **1** and AuNP **2**, respectively. Symbol key: *, Au^+ (*m/z* 197); @, Au_2^+ (*m/z* 394); #, the molecular ion corresponding to the headgroup fragment of phosphatidylcholine (*m/z* 184).

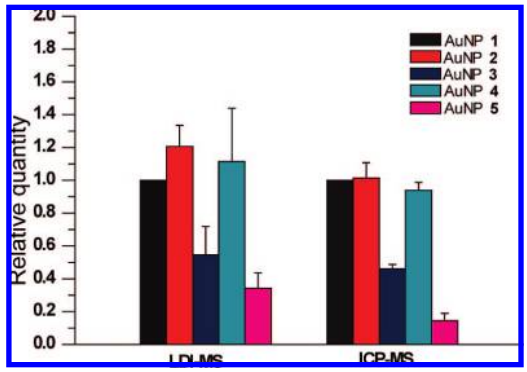

Figure 4. Relative quantities of the AuNPs in COS-1 cell lysates determined by LDI-MS and ICP-MS. In both cases, the AuNP amounts are normalized to that of AuNP **1**.

of time before analysis by LDI-MS. As an example, equal amounts of AuNP **1** and AuNP **2** (300 pmol each) were incubated with cell lysate for different amounts of time, and the relative ratios between the two nanoparticles were found to remain steady for up to 24 h (Figure S4 in the Supporting Information), which indicates that these two nanoparticles have essentially the same stability in a cellular environment.

We also investigated the sensitivity of our LDI-MS approach by culturing COS-1 cells with differing amounts of AuNPs. We found that AuNPs present at levels as low as 30 pmol (50 nM)

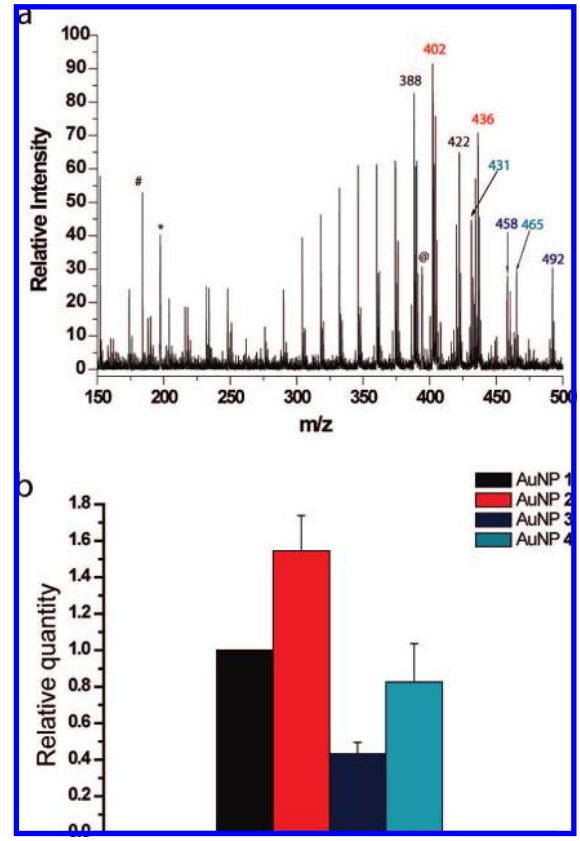

Figure 5. (a) Multiplexed LDI mass spectrum of COS-1 cell lysate with the four cationic AuNPs **1**−**4**. *m/z* 422, *m/z* 436, *m/z* 492, and *m/z* 465 correspond to AuNP **1**, AuNP **2**, AuNP **3**, and AuNP **4**, respectively. The symbol key is the same as in Figure 3. (b) Relative amounts of AuNPs **1**−**4** obtained from LDI-MS. The AuNP amounts are normalized to that of AuNP **1**.

in cell cultures could be readily detected. Figure S5 (Supporting Information) illustrates this for experiments with AuNP **1**. The characteristic peak for AuNP **1** is readily apparent, *m/z* 422, with a signal-to-noise ratio of 75. With such a good signal, we feel that the AuNPs could be detected even when present at even lower amounts.

A key advantage of the LDI-MS measurements over the ICP-MS measurements or other measurements is the ability to simultaneously identify and quantitate the uptake of multiple AuNPs. To demonstrate the advantages of such a multiplexed analysis, COS-1 cells were cultured with four cationic AuNPs (AuNPs **1**−**4**) (300 pmol each), and the resulting cellular contents were analyzed by LDI-MS (Figure 5a). Diagnostic molecular ion peaks at *m/z* 422, *m/z* 436, *m/z* 492, and *m/z* 465 indicate the presence of AuNP **1**, AuNP **2**, AuNP **3**, and AuNP **4**, respectively. The relative quantities of each AuNP (Figure 5b and Table S2 in the Supporting Information) indicate that AuNP **2** is the most readily taken up by the cells, while AuNP **3** is the least readily taken up, quite similar to the results in Figure 4. The slight differences might be explained by the greater total concentrations of AuNPs present in the experiments giving rise to Figure 4. These greater concentrations may have increased the cell uptake competition between the AuNPs, causing AuNP **4**, for example, to be taken up less readily.

Conclusion

We have described the use of AuNPs with mass barcodes for the multiplexed screening of AuNP cellular uptake. We

demonstrate that the relative quantities of four different AuNPs taken up by cells can be simultaneously determined using LDI-MS with this approach. We also find that the cellular uptake of the functionalized AuNPs is dependent on the NP surface functionality, suggesting that differential cellular uptake and specific cell targeting might be possible if the appropriate surface functionalities are chosen. In the future, we plan to use this technique to evaluate differential AuNP uptake by different cell states (e.g., normal and diseased). A future improvement will be to combine the LDI-MS approach with subcellular fractionation. This combination should be able to identify the intracellular targets for the AuNPs. On the whole, this LDI-MS technique has great potential for both the development of AuNP-based delivery vectors and probing transport of nanomaterials in vitro and in vivo.

Experimental Section

All chemicals were obtained from Sigma-Aldrich (St. Louis, MO) unless otherwise noted.

AuNP 1−5 Synthesis. The Brust−Schiffrin two-phase synthesis method[31,44] was used for synthesis of AuNPs with core diameters around 2 nm (see Figure S6 in the Supporting Information). After that, the Murray place-exchange method was used to obtain functionalized AuNPs **1**−**5**[30,32] (see the Supporting Information for details).

Cell Culture and Cellular Uptake of AuNPs. Monkey kidney COS-1 cells (75 000 cells/well) were grown on a 24-well plate in high-glucose Dulbecco's modified Eagle's medium (DMEM; glucose (4.5 g L^{-1})) containing 4-(2-hydroxyethyl)-1-piperazineethanesulfonic acid (HEPES) buffer (pH 7.4, 25 mM) supplemented with fetal bovine serum (FBS; 10%). Cultures were maintained at 37 °C under a humidified condition with 5% CO_2. After 24 h of plating, the cells were washed once with cold PBS, and the solutions of nanoparticles (Table S3 in the Supporting Information) were added. Following 6 h of incubation, the cells were washed three times with PBS to remove extra nanoparticles and lysed for 15 min with a lysis buffer according to the kit from GENLANTIS. A quick freeze/thaw cycle (freeze for 2 h at −20 °C and then thaw at room temperature) was performed to improve lysis. The lysed cells were then prepared for LDI-MS or ICP-MS analyses. For screening of four cationic nanoparticles (AuNPs **1**−**4**) simultaneously, the COS-1 cells were plated on a six-well plate with 75 000 × 4.8 cells/well. The cells were treated in a manner similar to that mentioned above. A mixture of four AuNPs (Table S3 in the Supporting Information) was added to each well and incubated for 6 h.

Control Experiments for Quantification. COS-1 cells were first lysed, and then the solutions of nanoparticles in PBS only (Table S4 in the Supporting Information) were added to each well and kept in the incubator for 6 h. The amount of nanoparticles and sample preparations were the same as described above except that no medium was added.

Cell TEM. Cells were treated with AuNP **1** (1 μM NP in a 600 μL solution per well in a 24-well plate) and washed with PBS buffer after 6 h. Then the cells were removed from the plate by trypsinization and centrifuged to collect the pellet. The pellet was fixed with 2% gluteraldehyde for 30 min and postfixed with 1% OsO_4 for 1 h. *OsO_4 is highly poisonous and must be used with extreme caution!* Following agarose (1.5%) enrobing, Spurr's resin embedding, and ultrathin (50 nm) sectioning, the samples were stained with 2% aqueous uranyl acetate and 25 mg/mL lead citrate and imaged with a JEOL 100S microscope.

LDI-MS Instrumentation. Most of the LDI-MS analyses were done on a Bruker Reflex III time-of-flight mass spectrometer. Only the sensitivity experiments (Figure S5 in the Supporting Information) were performed on a Waters Micromass M@LDI L/R mass spectrometer. The Bruker Reflex III is equipped with a 337 nm nitrogen laser, a 1.0 m flight tube, and a stainless steel sample target. All mass spectra were acquired in reflectron mode using a voltage of 16 kV. All reported spectra represent an average of 50 shots acquired at 90% laser power. The accelerating voltage was set to 20 kV. The Waters instrument was operated in positive reflection mode. The pulse voltage was set to 2400 V, the source to 15 000 V, and MCP to 1850 V. Matrix suppression delay was set to m/z 100. The spectrum represents an average of 50 shots acquired at 70% high laser power.

LDI-MS Sample Preparation and Measurements. The lysed cells were centrifuged at 14 000 rpm for 10 min. AuNPs precipitated together with the cell lysates were washed with 60% acetonitrile/40% water, applied directly to a stainless steel target, and allowed to dry. The dry samples were washed with 60% acetonitrile/40% water and then allowed to dry before LDI analysis. Each AuNP experiment was performed in triplicate, and at least five spots of each replicate were measured by LDI-MS.

ICP-MS Instrumentation. All ICP-MS measurements were performed on a Perkin-Elmer Elan 6100. Operating conditions of the ICP-MS are listed below: rf power, 1200 W; plasma Ar flow rate, 15 L/min; nebulizer Ar flow rate, 0.96 L/min; isotopes monitored, ^{197}Au and ^{103}Rh (as an internal standard); dwell time, 50 ms; nebulizer, cross-flow; spray chamber, Scott.

ICP-MS Sample Preparation and Measurements. Each AuNP was incubated with COS-1 cells separately as described above (Table S3 in the Supporting Information). After incubation and lysing of the cells, the resulting cell lysate was digested overnight using 3 mL of HNO_3 and 1 mL of H_2O_2. On the next day, 3 mL of aqua regia was added, and then the sample was allowed to react for another 1−2 h. *Aqua regia is highly corrosive and must be used with extreme caution!* A hot plate (∼100 °C) was used to reduce the above digested solution to 1−2 mL. The concentrated sample solution was then diluted to 100 mL with deionized water, and aqua regia and a ^{103}Rh internal standard solution were also added. The final AuNP sample solution contained 5% aqua regia and 10 ppb ^{103}Rh. The AuNP sample solution was measured by ICP-MS under the operating conditions described above. Cell uptake experiments with each AuNP were repeated 3 times, and each replicate was measured 10 times by ICP-MS. A series of gold standard solutions (20, 10, 5, 2, 1, 0.5, 0.2, and 0 ppb) were prepared before each experiment. Each gold standard solution contained 5% aqua regia and 10 ppb ^{103}Rh. Each standard solution was measured 10 times by ICP-MS using the operating conditions described above. The resulting calibration line was used to determine the gold amount taken up by the cells in each sample. A ∼100 ppm solution of dithiothreitol was used to wash the instrument between analyses to facilitate gold removal.

Acknowledgment. This work is supported by the Office of Naval Research under Award No. N000140510501 (R.W.V. and V.M.R.), the NIH (Grant GM077173, V.M.R.), and the NSF Center for Hierarchical Manufacturing (Grant DMI-0531171). We thank Prof. Julian F. Tyson and Dr. Elena Dovova for access to and assistance with the ICP-MS instrumentation and Dale A. Callaham for help with TEM imaging.

Supporting Information Available: Description of the synthesis of the gold nanoparticles, more detailed experimental protocols, and additional LDI-MS and ICP-MS data. This material is available free of charge via the Internet at http://pubs.acs.org.

JA805392F

(44) Brust, M.; Walker, M.; Bethell, D.; Schiffrin, D. J.; Whyman, R. *J. Chem. Soc., Chem. Commun.* **1994**, 801–802.